JOURNAL OF EXPERIMENTAL AND THEORETICAL PHYSICS, 2024, Vol. 165, No. 5, pp. 672–679

## ORDER, DISORDER, AND PHASE TRANSITION IN CONDENSED MEDIA

# EXCHANGE BIAS VARIATIONS AND MAGNETIC ANISOTROPY OF FILM STRUCTURES BASED ON FeMn ANTIFERROMAGNET

© 2024 V. O. Vas'kovskiy [a, b], A. A. Bykova [a, *], A. N. Gorkovenko [a], M. E. Moskalev [a], V. N. Lepalovskij [a]

[a] *Ural Federal University named after the First President of Russia B. N. Yeltsin, 620002, Yekaterinburg, Russia*
[b] *Mikheev Institute of Metal Physics*
*Ural Branch of the Russian Academy of Sciences, 620990, Yekaterinburg, Russia*
** e-mail: nastyabykowa@gmail.com*

Received August 23, 2023
Revised December 28, 2023
Accepted January 03, 2024

**Abstract**. The results of a systematic experimental study of FeNi/FeMn/FeNi film composites hysteresis properties are presented in conditions of varied thickness of the antiferromagnetic FeMn layer, temperature, and magnetic background. It is shown that the influence of these factors on coercive force and exchange bias field can be explained based on the concepts of highly dispersed polycrystalline structure of the antiferromagnetic layer. An original method for evaluating the temperature dependence of antiferromagnet magnetic anisotropy constant of the magnetic anisotropy constant of antiferromagnet has been implemented.

**DOI:** 10.31857/S004445102405e067

## 1. INTRODUCTION

In recent decades, considerable attention in the physics of composite materials has been paid to the study of magnetic systems that include exchange-coupled layers of antiferromagnetic and ferromagnetic metals. The exchange interaction that arises between the layers leads to a certain correlation of their magnetic structures. And the absence of spontaneous magnetization in the antiferromagnet and, consequently, its response to a relatively small magnetic field induces unidirectional magnetic anisotropy in the frromagnet, manifesting in a shift of its hysteresis loop along the magnetic field axis. This effect, called exchange bias, is of interest for such promising scientific and technical directions as spintronics, magnetic sensing, magnetic information processing [1–4].

This effect was first discovered in 1956 during the study of single-domain Co particles coated with antiferromagnetic CoO oxide [5, 6], and since then, a large amount of information has been accumulated on the implementation and features of exchange bias in various ferro-/antiferromagnetic composites [7–9]. A classic example of composites demonstrating the exchange bias effect is polycrystalline films of type, FeMn/FeNi, containing a ferromagnetic permalloy layer and an antiferromagnetic layer $Fe_{20}Ni_{80}$ and an antiferromagnetic layer $Fe_{50}Mn_{50}$. The functional properties of this structure are limited by a relatively low blocking temperature ($T_b \leqslant 400$ *K*) [10]. However, it has its advantages, which include the relative simplicity of exchange bias implementation, good reproducibility of its parameters, and, of course, the absence of expensive elements such as Ir or Pt in the antiferromagnet composition [11]. A significant number of studies have been devoted to examining the structure of type FeMn/FeNi, which established patterns of exchange bias formation while varying the thicknesses of ferromagnetic and antiferromagnetic layers, composition of buffer layers, interfacial roughness, temperature, magnetic history, and thermomagnetic treatment conditions [12–18]. This includes establishing the role of epitaxial growth effect in achieving optimal crystalline structure and texture of composites; determining critical thickness parameters of the layered structure; identifying features of thermally activated interlayer diffusion; and demonstrating that many characteristic features of hysteresis properties are caused by dispersion in the crystallite size of the antiferromagnetic layer.

Thus, FeMn/FeNi film composites appear to be a well-studied carrier of the exchange bias effect and in this regard can be considered as a model object, highly suitable for testing new approaches to experimental study of such media, as well as constructing their physical and computer models. In particular, it is of interest to evaluate the effectiveness of using such bilayers for indirect determination of the magnetic anisotropy constant of the antiferromagnetic component. The quantitative description of antiferromagnetic anisotropy itself is a challenging task. The absence of spontaneous magnetization places very high demands on the implementation of traditional methods used in this field. Within their framework, to determine the magnetization anisotropy [19] or resonant microwave absorption conditions [20], ultra-strong stationary magnetic fields (with intensity more than $10^5$Oe) and ultra-high-frequency electromagnetic radiation (with frequency more than $10^2$ GHz) are required, i.e., complex experimental equipment. The situation is complicated by the fact that for qualitative interpretation of magnetization curves or effective magnetic field components obtained through these methods, single-crystal samples of sufficient volume must be used in the experiment. Incomparably more accessible is the method for determining the antiferromagnetic anisotropy constant, proposed in [21] when studying polycrystalline films of type IrMn /FeNi and known as the York protocol. It is based on analyzing the exchange bias field dependencies on the magnetic history of samples and allows determining the anisotropy constant of IrMn antiferromagnet at one fixed temperature.

This work is devoted to the physical justification of the possibility of applying the York protocol for determining the temperature behavior of the antiferromagnetic magnetic anisotropy constant, which is based on a detailed analysis of the exchange bias effect in polycrystalline films of type FeMn/FeNi with different thicknesses of the antiferromagnetic layer.

## 2. DESCRIPTION OF EXPERIMENTAL METHODS

Multilayer films of glass /Ta(5)/$Fe_{20}Ni_{80}$(5)/FeMn($L$)/$Fe_{20}Ni_{80}$(40) with variable thickness of the antiferromagnetic layer $L$ were studied, which were obtained by magnetron sputtering using the ATC Orion 8 system. The film structure formation occurred through sequential sputtering of single-component (Ta) or alloy targets of corresponding composition. The entire technological process was carried out at argon pressure $10^{-3}$ mm Hg in the presence of a uniform magnetic field (technological field) with intensity 250 Oe, oriented parallel to the sample plane, and with high-frequency electrical bias of 14 W applied to the substrate.

In the selected type of film composites, the Ta layer and the following permalloy layer (auxiliary layer) with thicknesses of 5 nm each had a structure-forming purpose and together, due to the epitaxy effect, should initiate the formation of FeMn crystallites with FCC lattice and (111) crystal texture. It is in this structural modification that FeMn exhibits antiferromagnetism and is a source of exchange bias [22].

The outer permalloy layer with a thickness of 40 nm (main layer) was functional. Its hysteresis properties were mainly used to indicate the magnetic state of the FeMn layer. Additionally, both ferromagnetic layers together provided supplementary information about the pinning properties of different surfaces of the antiferromagnetic layer. The prerequisite for this was the significant difference in thickness between the permalloy layers, which allowed to "separate" their magnetization reversal fields. The nominal thickness of the FeMn layer varied within 2–20 nm and, as with other layers, was controlled in the film structure composition by time and pre-determined metal deposition rates. The error of this certification method is estimated by us to be $\pm 0.2$ nm.

Structural characterization of the obtained multilayer films was performed using a Bruker D8 ADVANCE diffractometer in Cu$K_a$ radiation. For certification of films by magnetic properties at room temperature and in the temperature range $5 \leqslant T \leqslant 400$ K, a Kerr magnetometer Evico magnetics and PPMS DynaCool T9 measurement complex were used respectively.

## 3. RESULTS AND COMMENTS

Fig. 1 shows the diffractometry results for a series of samples with different FeMn layer thicknesses. Using the example of a film with $L = 20$ based on the diffractogram containing only two reflections, one can conclude that it contains two main phases with FCC lattice, parameters $a$ of which are 0.3598

and 0.3541 nm. They can be identified respectively with FeMn and FeNi layers, textured by type (111), thus confirming the realization of the necessary structural state. However, with decreasing $L$ the diffraction reflection from FeMn becomes less pronounced and eventually ceases to be resolved. At the same time, the FeNi line remains practically unchanged. Obviously, it is formed predominantly by the outer permalloy layer with greater thickness, and the stability of its structural state indicates, among other things, the presence of through texture of type (111) in all studied samples.

The general characterization of the magnetic state of the entire sample series can be given based on Fig. 2, which shows the dependences of coercive force $H_c$ (hysteresis loop half-width) and exchange bias field $H_e$ (magnitude of hysteresis loop center shift along the field axis) of both permalloy layers on the FeMn layer thickness. The values of these parameters were determined from magneto-optical hysteresis loops measured at room temperature from both sides of the films. As known, the magnitude and sign of the field $H_e$ can depend on the magnetic history of samples [23, 24]. Therefore, for certainty, all measurements were performed immediately after film preparation, which was carried out in a technological field of conditionally negative sign.

The presented data show that the FeMn layer begins to significantly manifest itself at a thickness greater than 2.5 nm, causing an intensive increase in the coercive force of ferromagnetic layers. It continues within a rather narrow interval $L$, and then changes to a more gradual decrease $H_c$ with followed by stabilization at a steady level, which, however, is significantly higher than the coercive force characteristic of single-layer films of corresponding thicknesses (about 1 Oe). Overall, the dependencies $H_c(L)$ for the main and auxiliary FeNi layers are qualitatively similar but differ significantly in quantitative terms. The latter can largely be attributed to the difference in layer thicknesses and can be considered as evidence of the presence of a surface source of magnetization reversal delay. It should also be noted that there is a certain shift between the two presented curves along the

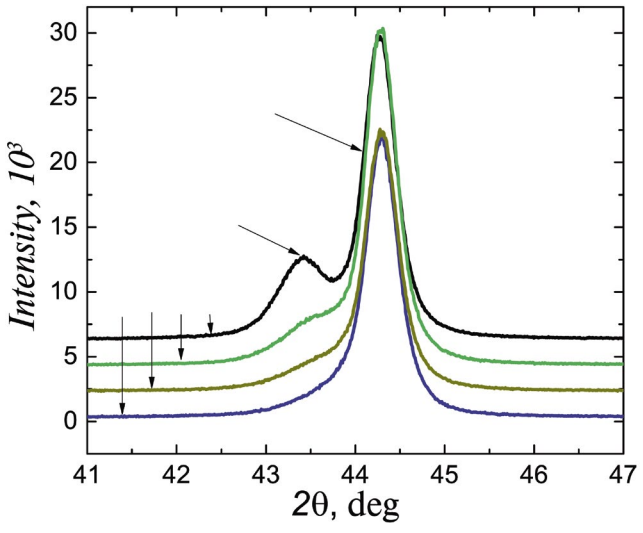


**Fig. 1.** Diffractograms of film structures with different FeMn layer thicknesses: $L$ = 5 (1), 7.5 (2), 10 (3), 20 (4) nm

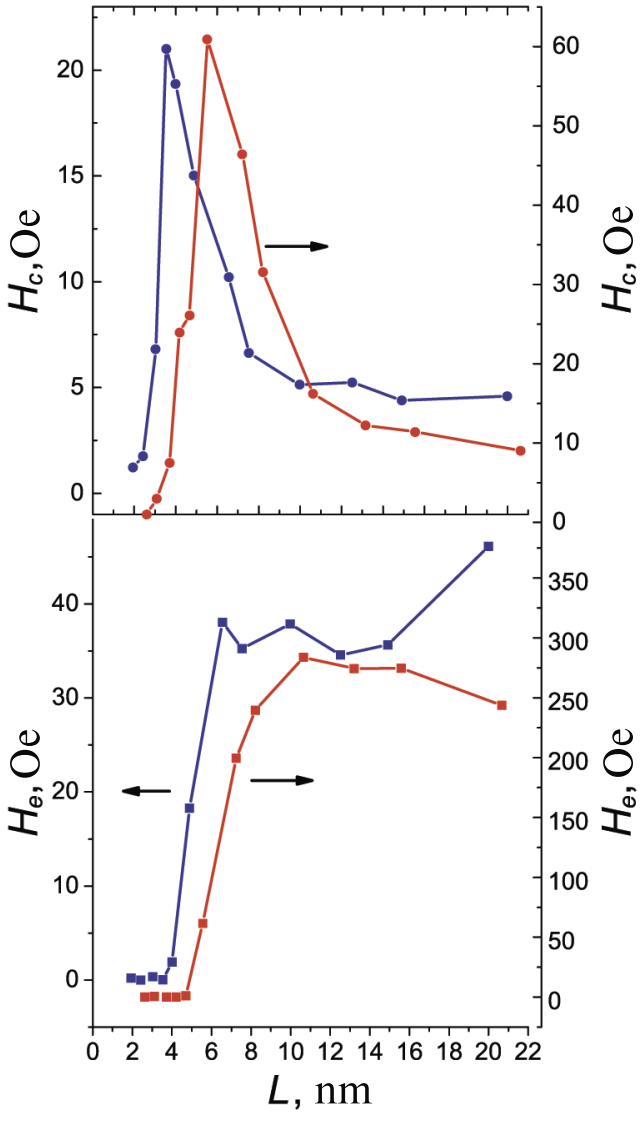


**Fig. 2.** Dependencies of coercive force (*a*) and exchange bias field (*b*) of the main (curves 1) and additional (curves 2) permalloy layers on the FeMn layer thickness

thickness axis. It shows a delay in the formation of magnetic hysteresis in the auxiliary layer relative to the main layer, which apparently reflects differences in the structural conjugation of the layers.

The exchange bias effect appears at $L > 4$ nm, occurring almost synchronously in both ferromagnetic layers. With increasing FeMn layer tickness, the exchange bias field $H_e$ rapidly increases and then reaches a relatively stable level in the range of 6–10 nm. Notably, in the auxiliary permalloy layer, as in the case of $H_c$, this occurs with a shift towards higher $L$. The exchange bias field values differ accordingly – for the auxiliary layer, the final level $H_e$ is much higher than for the main permalloy layer. The evaluation of the interlayer coupling constant $K_s$ at different interfaces shows that the noted difference is almost entirely a consequence of the different thicknesses of the ferromagnetic layers. Calculations performed using the formula $K_s = H_e$ ($L = 10$ nm) $M_s L_f$ [24], where $M_s$ is the spontaneous magnetization of permalloy, and is the thickness of the ferromagnetic layer, gave values of 0.12 and 0.11 erg/cm for the main and auxiliary layers respectively. Thus, in terms of exchange coupling efficiency, both interfaces are similar, which is indirect evidence of the uniformity of FeMn layer properties across its thickness.

The described patterns of formation $H_c$ and $H_e$ are similar to those given in [7] for films of type Cu/FeNi/FeMn($L$), and can be interpreted within the model of a polycrystalline antiferromagnet with weak intercrystallite exchange and exchange-coupled with ferromagnetic layers. In this model, the stability of the antiferromagnetism vector of each crystallite to thermal fluctuations and the influence from the magnetizing ferromagnetic layer, with which there is a direct exchange coupling, is important. Such stability is determined by the magnitude of anisotropy energy, i.e., the product of the anisotropy constant and crystallite volume. Based on this, all crystallites of the FeMn layer can be divided into three categories: conditionally "superparamagnetic", "magnetically unstable", and "stable". The first ones have a blocking temperature lower than the measurement temperature, and they practically do not affect the magnetization reversal process of ferromagnetic layers. The second ones are themselves in a stable state but change the orientation of the antiferromagnetism vector under the influence of ferromagnetic layers. Such crystallites form $H_e$, but do not create exchange bias. And finally, the third ones possess the highest stability of magnetic state, which is not affected by the above-mentioned influences. They determine $H_e$.

Within this division, the experimental dependencies $H_c(L)$ and $H_e(L)$ can be interpreted, considering that the increase in antiferromagnetic layer thickness leads to growth in average crystallite volume and gradual redistribution between the categories mentioned above. At $L < 2.5$ nm, if crystallites exist, they are in a "superparamagnetic" state at room temperature. In samples with slightly larger $L$, some crystallites are "magnetically unstable," which leads to increased coercivity. Then crystallites of the third category appear, which provide exchange bias. It is characteristic that the maxima of $H_c$ (see Fig. 2) are localized approximately in the middle of the intervals $L$, where sharp changes in $H_e$ of ferromagnetic layers occur. At such thicknesses, apparently, there is some parity in the concentrations of "magnetically unstable" and "stable" crystallites.

The presented interpretation of hysteresis properties of films FeNi/FeMn/FeNi with different thicknesses of the antiferromagnetic layer is confirmed by the results of temperature studies. Figure 3 shows the most characteristic dependencies of $H_c(T)$ and $H_e(T)$ of the main permalloy layer for several values of $L$. They were determined from magnetometric hysteresis loops during monotonic heating of samples from 5 to 300 K. Cooling to the initial temperature was carried out in a conditionally negative magnetic field (corresponding to the sign of the technological field) with intensity of 5 kOe state "N". In this state, magnetic preparation was carried out by single cyclic magnetization reversal of samples in a magnetic field with amplitude of 5 kOe. Then, at this and subsequent temperatures, hysteresis loops were measured, parameters of which were used for analysis. Transition from one temperature to another occurred in the maximum magnetization reversal field (5 kOe) of negative sign. The duration of one measurement cycle, including temperature stabilization time, was about 30 minutes. From Figure 3*a* it can be seen that at 5 K exchange bias is present in all studied samples, and for nm its effectiveness practically does not depend on the thickness of the FeMn layer. In the film with $L = 2$ nm, the value of $H_e$ is much lower than in other samples. This may be due to discontinuity of the thinnest FeMn layer or its

partial amorphization, accompanied by transition to paramagnetic state. Interestingly, curves 1 and 2 have a concave character, demonstrating more sharp changes in $H_e(T)$ in the region of $T < 50$ K. In general, such behavior of $H_e(T)$ can be interpreted as a reflection of segregation of antiferromagnetic crystallites by size into two dominant groups with blocking temperatures of 50 and 150 K. In other samples, the dependencies of $H_e(T)$ are convex and demonstrate decrease in temperature sensitivity of exchange bias field with increase in $L$ up to 8 nm, after which thickness stabilization of properties occurs.

The coercive force behaves accordingly (Fig. 3*b*). In samples with small $L$ it is generally higher and shows non-monotonic temperature dependence (curves 2, 3, 4), in particular, the presence of a maximum that shifts to higher temperatures with increasing $L$. The maximum is localized in the temperature range where exchange bias appears. In terms of the aboveintroduced gradation of the magnetic state of FeMn crystallites, this means that as temperature decreases, a significant portion of them sequentially transitions from the "superparamagnetic" category to "magnetically unstable" and "stable" categories. Accordingly, $H_c$ first increases and then decreases. In samples with $L \geqslant 10$ nm, the coercive force changes little over a wide temperature range (curve 5), indicating that the main part of antiferromagnetic crystallites belongs to the "stable" category. However, near helium temperatures, the behavior of $H_c(T)$ changes, showing quite sharp growth in all samples without exception.

From this, we can conclude that FeMn layers almost always contain, to some extent, an ultrathin superparamagnetic phase with a blocking temperature of 50 K, which does not contribute to exchange bias, i.e., its crystallites do not transition to the "stable" category in principle. There is also a version suggesting that this phase consists of intercrystallite layers in a "spin glass"-like state [25] with a freezing temperature below 50 K. Additionally, we note that the hysteresis properties of the auxiliary permalloy layer change with temperature in a qualitatively similar manner.

As a continuation of this experiment, similar temperature measurements of hysteretic properties were conducted on the same samples from the initial state, obtained by cooling in a magnetic

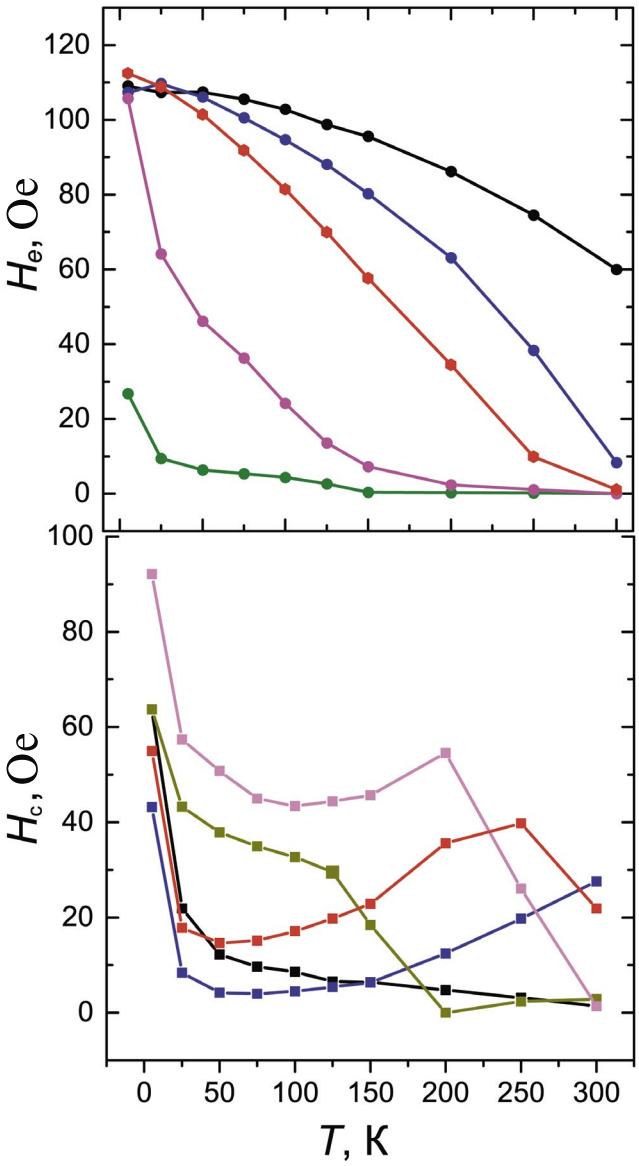


**Fig. 3.** Temperature dependencies of exchange bias field (*a*) and coercive force (*b*) of the main permalloy layer for films with different FeMn layer thickness, obtained from the "N" state: $L$ = 2(1), 3(2), 4(3), 5(4), 20(5) nm

field of opposite sign (opposite to the sign of the technological field) – state "P". In the same field, the samples were kept while varying the temperature. The corresponding dependencies $H_e(T)$ are shown in Fig. 4. As can be seen, they underwent significant changes compared to the data obtained in state "N". In all samples that did not possess significant exchange bias at room temperature ($L \leqslant 5$ nm), the field $H_e$ acquired a different sign while maintaining the character of temperature behavior (curves 1–4). For films with larger $L$ the sign $H_e$ remained unchanged, but the dependencies

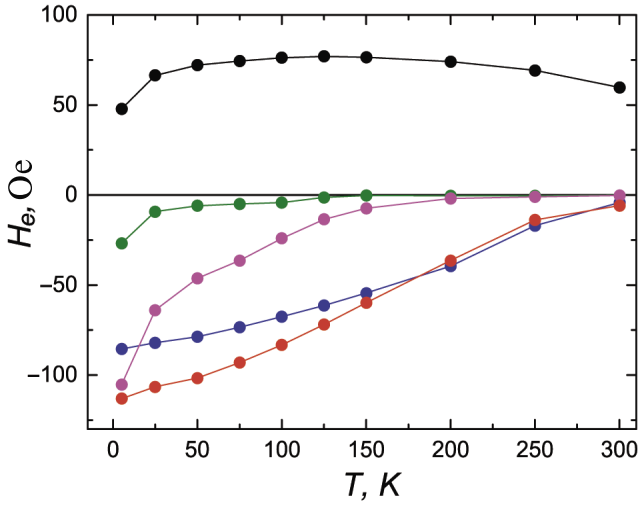


**Fig. 4.** Temperature dependencies of the exchange bias field of the main permalloy layer for films with different FeMn layer thicknesses, obtained from state "P": $L$ = 2(1), 3(2), 4(3), 5(4), 20(5) nm

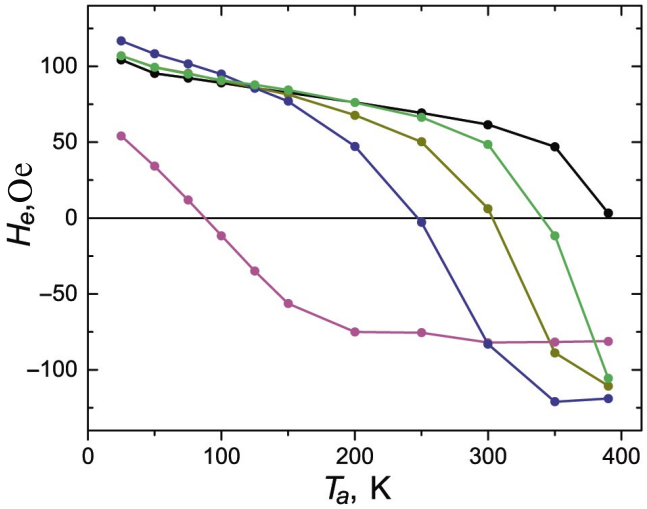


**Fig. 5.** Dependencies of the exchange bias field of the main permalloy layer on activation temperature for films with different FeMn layer thicknesses: $L$ = 3(1), 5(2), 7.5(3), 10(4), 20(5) nm

$H_e(T)$ became non-monotonic (curve 5). All these changes fit into the above-described model of a structurally inhomogeneous antiferromagnet. In samples with $L \leqslant 5$ nm, "superparamagnetic" and "magnetically unstable" crystallites, transitioning to the "stable" category during cooling, fix the new position of the ferromagnetic layer magnetization, leading to a corresponding shift in its hysteresis loop. As temperature increases, the number of such crystallites at the interlayer interface decreases, leading to a reduction in the absolute value of $H_e$. In films with a thicker FeMn layer, the proportion of crystallites changing their state depending on magnetic prehistory is relatively small. Therefore, in such samples during cooling, the exchange bias field does not change sign but only slightly decreases. Heating leads to the transition of this portion of crystallites to the "magnetically unstable" category. This initiates the growth of $H_e$ with temperature increase in the region $T < 100$ K. Note also that the temperature dependencies of coercive force obtained in this experiment practically completely reproduce the data presented in Fig. 3*b*, and thereby show weak dependence $H_c$ on the magnetic prehistory of the films.

More detailed information about the relationship between the structural and magnetic states of the FeMn layer can be obtained using the original methodology proposed in [21]. It consists in determining the so-called median blocking temperature $\langle T_b \rangle$ and subsequent calculation of the antiferromagnetic anisotropy constant based on this. The York protocol is designed to obtain quantitative results and requires fairly strict adherence to measurement procedures that ensure the occurrence of main relaxation processes in the magnetic state of films. In our case, measurements were carried out according to the following scenario: cooling the sample to 25 K in a negative magnetic field (-5 kOe) → magnetic preparation → measurement of hysteresis loop → heating in a positive magnetic field (+5 kOe) to a specific activation temperature $T_a$, holding for 1 hour (activation time), cooling to 25 K magnetic preparation → measurement of hysteresis loop → repetition of the measurement cycle with heating to a higher activation temperature. The value $T_a$ was increased in steps of 25 K up to a temperature of 400 K.

Fig. 5 shows the dependencies of the exchange bias field of the main permalloy layer on the activation temperature for samples with different $L$. As can be seen, all curves are monotonically decreasing and demonstrate a sign change of $H_e$. Such behavior $H_e(T_a)$ reflects the fact that part of the antiferromagnetic crystallites that lost stability at elevated temperature returns to the "stable" category upon subsequent temperature decrease, changing the orientation of the antiferromagnetism vector. This occurs due to the exchange action from the ferromagnetic layer with a magnetization orientation different from the initial one. The activation temperature, after heating to which the

exchange pinning from two groups of crystallites with different orientations of the antiferromagnetism vector balances out and $H_e$ turns to zero, is taken as the median blocking temperature $\langle T_b \rangle$.

Overall, the dependence $\langle T_b \rangle$ on the FeMn layer thickness is shown in Fig. 6*a*. Its ascending character once again indicates an increase in the average size and, accordingly, the anisotropy energy of antiferromagnetic crystallites, which is determined by the expression $E_a = KV$, where $K$ – is the magnetic anisotropy constant of the antiferromagnet, $V$ is the crystallite volume. Information about $\langle T_b \rangle$ allows estimating the value of $K$, for which, following the authors of work [21], one can use the relation

$$K(\langle T_b \rangle) = \frac{\ln(tf_0)}{\langle V \rangle} k \langle T_b \rangle,$$

where $k$ – is the Boltzmann constant, $t$ – is the magnetic relaxation time, which was taken as the activation time (1 hour), $f_0$ is the characteristic frequency of magnetic moment switching, which according to estimate [25] is $2.1 \cdot 10^{12}$ Hz, $\langle V \rangle$ – is the average crystallite volume. To determine $\langle V \rangle$, a cylindrical crystallite approximation was adopted with height equal to the thickness of antiferromagnetic layers and fixed base area. The basis for such approximation is the known data about the columnar nature of the microstructure of metallic films obtained by magnetron sputtering [26]. The cross-sectional area of cylindrical crystallites was determined by the average diameter, calculated from X-ray data using the Scherrer formula [27]. For this purpose, diffractogram 4 in Fig. 1 was used, where the FeMn line was isolated by approximating the real curve with two Gaussian functions. As a result, a value of 6 nm was obtained and used in calculations.

The above formula connects the calculated value of the anisotropy constant with a specific value of $\langle T_b \rangle$. The set of such data for a series of $\langle T_b \rangle$, obtained on samples with different $L$ according to the York protocol (Fig. 6*a*), effectively gives the dependence of $K$ on temperature [28]. The corresponding graph is shown in Fig. 6*b*. As can be seen, the dependence $K(T)$ has a monotonically decreasing character, typical for most magnetically ordered substances. Moreover, the magnitude level of the obtained data correlates well with the results presented in [29,30]. Both factors to some extent indicate the adequacy

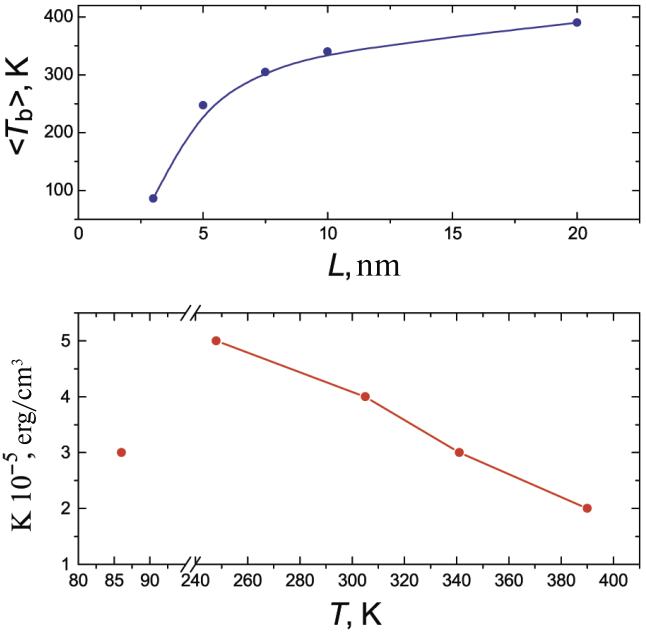


**Fig. 6.** Dependencies of the median blocking temperature on the FeMn(*a*) layer thickness and magnetic anisotropy constant FeMn(*b*) on temperature

of the methodological approach used. The exception is the result obtained for the sample with $L = 3$ nm, which has a concave dependence $H_e(T)$ (curve 1 in Fig. 5). It is shown in Fig. 6*b* as a separate point. Probably, at this and smaller thicknesses of the antiferromagnetic layer, the polycrystalline model of its structural state is not entirely acceptable.

## 4. CONCLUSION

The conducted research provides comprehensive confirmation of the highly dispersed polycrystalline antiferromagnet model responsible for the formation of hysteresis properties, including exchange bias, in layered film composites of ferromagnet/antiferromagnet/ferromagnet type. It is shown that the experimentally obtained dependences of coercive force and exchange bias field on the antiferromagnetic layer thickness, temperature, and magnetic prehistory find qualitative explanation through varying the ratio of three categories of antiferromagnetic crystallites: "superparamagnetic", "magnetically unstable", "stable". It is demonstrated that the application of a special measurement methodology (York protocol) to samples with different antiferromagnetic layer thicknesses allows determining the temperature dependence of the antiferromagnet's magnetic anisotropy constant.

## ACKNOWLEDGMENT

The authors express gratitude to N. V. Selezneva for diffractometry of the studied samples.

## FUNDING

This work was carried out with financial support from the Ministry of Education and Science of the Russian Federation, project FEUZ 2023 0020.

## REFERENCES

**1.** X. Chen, A. Hochstrat, P. Borisov et al., Appl. Phys. Lett. 89, 20 (2006).

**2.** C. H. Marrows, L. C. Chapon, and S. Langridge, Materials Today 12, 70 (2009).

**3.** E. Lage, C. Kirchhof, V. Hrkac et al., Nature Materials 11, 523 (2012).

**4.** J. Fassbender, S. Poppe, T. Mewes et al., Appl. Phys. A 77, 51 (2003).

**5.** W. H.Meiklejohn and C. P. Bean, Phys. Rev. 102, 1413 (1957).

**6.** E. D. Dahlberg, B. Miller, B. Hill et al., J. Appl. Phys. 83, 6893 (1998).

**7.** K. H. J. Buschow, Handbook of Magnetic Materials, Elsevier, North-Holland (2015).

**8.** S. Erokhin, D. Berkov, and A. Michels, arXiv: 2309.17131.

**9.** J. A. Calderon, H.P. Quiroz, C.L. Teran et al., Sci. Rep. 13, 722 (2023).

**10.** H. Sang, Y. W. Du, and C. L. Chien, J. Appl. Phys. 85, 4931 (1999).

**11.** J. Kanak, T. Stobiecki, and S. van Dijken, IEEE Trans. Magn. 44, 238 (2008).

**12.** P. Savin, J. Guzman, V. N. Lepalovskij et al., J. Magn. Magn. Mater. 402, 49 (2016).

**13.** A. V. Svalov, G. V. Kurlyandskaya, V. N. Lepalovskij et al., Superlattices and Microstructures 83, 216 (2015).

**14.** K. C. Chen, Y. H. Wuet al., J. Appl. Phys. 101, 9 (2007).

**15.** T. R. Gao, D. Z. Yang, S. M. Zhou et al., Phys. Rev. Lett. 99, 057201 (2007).

**16.** K. Y. Kim, H.C. Choi, J. H. Shim et al., IEEE Trans. Magn. 45, 2766 (2009).

**17.** M. F. Toney, C. Tsang, and H. Kent, J. Appl. Phys. 70, 6227 (1991).

**18.** J. B. Youssef, D. Spenato, H. L. Gall et al., J. Appl. Phys. 91, 7239 (2002).

**19.** N. V. Mushnikov, Magnetism and Magnetic Phase Transitions, Ural University Publishing (2017).

**20.** A. G. Gurevich, Magnetic Resonance in Ferrites and Antiferromagnets, Nauka, Moscow (1973).

**21.** K. O'Grady, L. E. Fernandez-Outon, and G. VallejoFernandez, J. Magn. Magn. Mater. 322, 883 (2010).

**22.** V. O. Vaskovsky, V. N. Lepalovsky, A. N. Gorkovenko et al., Technical Physics 85, 118 (2015) [V. O. Vas'kovskiy, V. N. Lepalovskij, A. N. Gor'kovenko et al., J. Techn. Phys. 60, 116 (2015)].

**23.** A. V. Svalov, E. V. Kudyukov, V.N. Lepalovskij et al., Current Appl. Phys. 23, 68 (2021).

**24.** V. O. Vas'kovskiy, A. N. Gorkovenko, N. A. Kulesh et al., Bulletin Russ. Acad. Sci. Phys. 83, 857 (2019).

**25.** N. A. Kulesh, M. E. Moskalev, V. O. Vas'kovskiy et al., Phys. Metals Metallogr. 122, 855 (2021).

**26.** J. A. Calderon, P. Q. Cristian, L. Teran et al., Sci. Rep. 13, 722 (2023).

**27.** P. Scherrer, Nach Ges Wiss Gottingen 2, 8 (1918).

**28.** M. E. Moskalev, PhD Thesis in Physics and Mathematics, UrFU, Yekaterinburg (2021).

**29.** J. De Clercq, A. Vansteenkiste, M. Abes et al., J. Phys. D: Appl. Phys. 49, 435001 (2016).

**30.** N. Koichi, H. Chunghong, F. Hideo et al., J. Appl. Phys. 80, 4528 (1996).